ACS Catalysis

Research Article

pubs.acs.org/acscatalysis

Computational Exploration of Mechanism and Selectivities of (NHC)Nickel(II)hydride-Catalyzed Hydroalkenylations of Styrene with α-Olefins

Xin Hong,[†] Jinglin Wang,[‡] Yun-Fang Yang,[†] Lisi He,[∥] Chun-Yu Ho,*[,‡,∥] and K. N. Houk*[,†]

[†]Department of Chemistry and Biochemistry, University of California, Los Angeles, California 90095, United States

[‡]Department of Chemistry, South University of Science and Technology of China (SUSTC), Shenzhen 518055, P.R. China

[∥]Shenzhen Research Institute, The Chinese University of Hong Kong, Shatin NT, Hong Kong, P.R. China

Supporting Information

ABSTRACT: The [LNiH]$^+$-catalyzed hydroalkenylation between styrene and α-olefins gives distinctive chemo- and regioselectivities with N-heterocyclic carbene (L = NHC) ligands: (a) the reaction with NHC ligands produces the branched tail-to-tail products, whereas the reaction with phosphine ligands (L = PR_3) favors the tail-to-head regio-isomers; (b) the reaction stops at heterodimerization with no further oligomerization even with excess α-olefin substrates; (c) typical side reactions with α-olefins, such as isomerization to internal olefins or polymerization, are either significantly diminished or eliminated. To understand the operating mechanism and origins of selectivities, density functional theory (DFT) calculations were performed, and several additional experiments were conducted. The olefin insertion step is found to determine both the regioselectivity and chemoselectivity, leading to the tail-to-tail heterohydroalkenylation product. With a small NHC ligand (1,3-dimethylimidazol-2-ylidene), the intrinsic electronic effects of ligand favor the tail-to-head regioisomer by about 1 kcal/mol in the olefin insertion step. With bulky NHC ligands (1,3-bis(2,6-dimethylphenyl)imidazol-2-ylidene or SIPr), the steric repulsions between the ligand and the substituent of the inserting alkene override the intrinsic electronic preference, making the tail-to-tail regioisomer favored (about 3 kcal/mol with both ligands). In the competition between homo- and heterodimerization, the insertion of the secondary styrene breaks its π-conjugation, making the insertion of styrene about 2 kcal/mol less favorable than that of alkyl-substituted alkenes. In addition, the interaction between nickel and phenyl group of styrene stabilizes the resting state and inhibits the side reactions with α-olefins, suggesting that styrene, or similar aryl olefins, is not only a substrate, but also an inhibitor for side reactions. This unique effect of styrene is verified by control experiments.

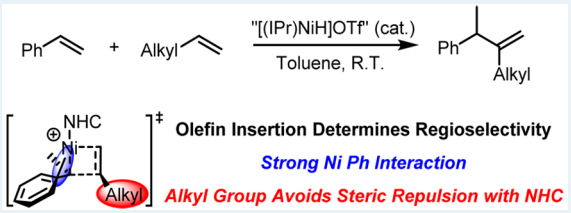

KEYWORDS: *hydrovinylation, regioselectivity, β-hydride transfer, NHC ligand, density functional theory*

INTRODUCTION

Efficient and selective carbon−carbon bond formation that uses abundant and renewable feedstock chemicals for the synthesis of valuable products is a major focus of modern synthetic chemistry.[1] Hydroalkenylations, which add a vinyl group and a hydrogen across a double bond, are atom and step economic when high reactivity and selectivity is achieved (Scheme 1).[2] Since the first report by Alderson in 1965,[3] many research groups have devoted efforts to the development of transition metal catalysts for this reaction.[4−9] The phosphorus-based nickel-hydride catalysts and their equivalents, contributed by Wilke,[10] RajanBabu,[11] Leitner,[12] and others,[13] have received the most attention for their high efficiency, chemo- and especially enantioselectivity.

Ho and co-workers recently reported that the in situ generated [(NHC)NiH]$^+$ catalyst can provide distinctive reactivities and selectivities in the hydroalkenylation between a variety of vinylarenes and α-olefins.[14] The NHC-ligated catalysts selectively facilitate the tail-to-tail heterohydroalkenylation, shown in Scheme 2b and 2c, producing the branched terminal 1,1-disubstituted alkenes.[14a,15] With phosphine ligands, the nickel-hydrides favor other regioisomers, as shown in Scheme 2a.[4b,c,16] In addition, the NHC ligands favor 1:1 adducts, with no further oligomerization even with excess α-olefins. Typical side reactions with α-olefins, such as the olefin isomerization, are also limited by NHC ligands.

Scheme 1. Chemo- and Regioselectivities in Hetero-Hydroalkenylation Reactions

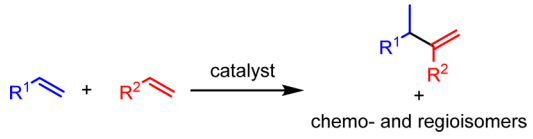

Received: May 22, 2015
Revised: August 9, 2015
Published: August 13, 2015

DOI: 10.1021/acscatal.5b01075
ACS Catal. 2015, 5, 5545−5555

Scheme 2. Regioselectivities of [(L)NiH]$^+$-Catalyzed Hetero-Hydroalkenylation between Styrene and α-Olefins: (a) L = Ph_3P, (b) L = IMes, (c) L = IPr

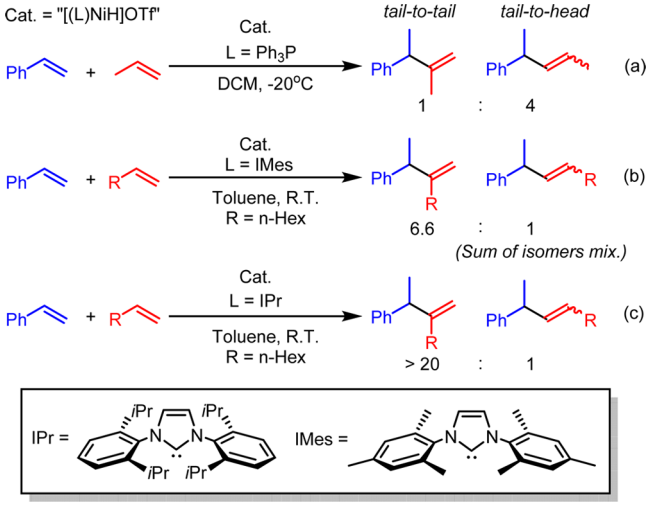

Despite the experimental and theoretical studies on the mechanism of [(R_3P)NiH]$^+$-catalyzed hydroalkenylation,[17] the origins of the intriguing reactivities and selectivities of the reactions involving the [(NHC)NiH]$^+$ catalysts are still unknown. We have undertaken a theoretical study to answer the following questions: What is the mechanism of hydroalkenylation with the [(NHC)NiH]$^+$ catalysts? What are the origins of the reactivities and selectivities of hydroalkenylation with these NHC-ligated nickel-hydride catalysts? Why do phosphine and NHC ligands, the two most popular types of ligands in nickel chemistry, produce such different regioselectivities in this reaction?

COMPUTATIONAL METHODS

Geometry optimizations, vibrational frequencies, and thermal energy corrections were performed with the B3LYP functional, and the 6-31G(d) basis set for all main group elements and SDD basis set for nickel as implemented in Gaussian 09.[18] Energies were evaluated with the M06 method,[19] the 6-311+G(d,p) basis set for all main group elements, and the SDD basis set for nickel. All reported free energies involve zero-point vibrational energy corrections and thermal corrections to Gibbs free energy at 298 K. The solvation free-energy corrections were computed with the SMD model[20] on gas-phase optimized geometries, and toluene was chosen as the solvent for consistency with the experiment. Extensive conformational searches for intermediates and transition states have been conducted, but only the most stable conformers and isomers are discussed here.

RESULTS AND DISCUSSION

Reaction Mechanism. The proposed mechanism for the [(NHC)NiH]$^+$-catalyzed hydroalkenylation of styrene and α-olefins is shown in Scheme 3. This mechanism is based on previous theoretical and experimental studies on the mechanisms of [LNiH]$^+$-catalyzed hydroalkenylation with phosphine ligands and other related reactions.[21] The initial hydride insertion of **1** produces the η^3-allylic nickel species **2**, and subsequent insertion of α-olefin gives the intermediate **4**. From **4**, the β-hydride elimination can occur to generate the heterodimer coordinated nickel complex **5**, and subsequent

Scheme 3. Tentative Mechanism Proposed for [(NHC)NiH]$^+$-Catalyzed Hydroalkenylation of Styrene and α-Olefins

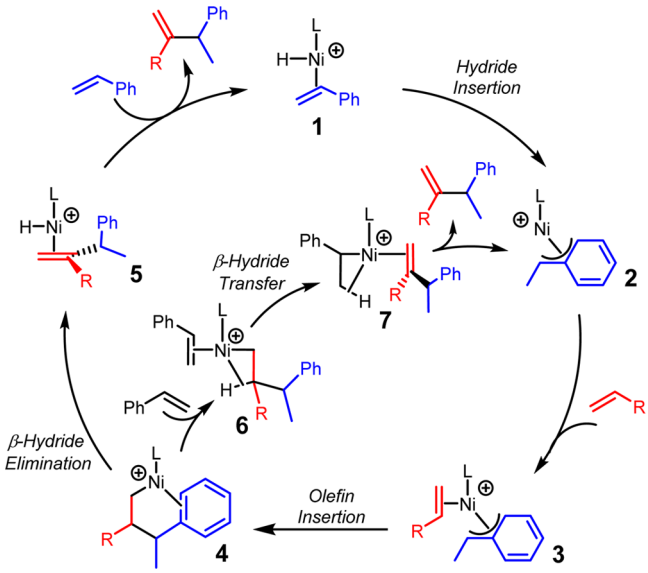

product extrusion produces the heterodimer product and regenerates **1**. Alternatively, **4** can undergo a styrene coordination to produce intermediate **6**, and subsequent β-hydride transfer and product extrusion produce the same heterodimer product and regenerate intermediate **2**.

We first studied the mechanism computationally, using the homodimerization of styrene as an example and 1,3-bis(2,6-dimethylphenyl)imidazol-2-ylidene as the model NHC ligand.[22] The free-energy changes of the most favorable pathway are shown in Figure 1. From [LNiH(styrene)]$^+$ complex **8**, a facile hydride insertion on the terminal carbon of styrene occurs via **TS9** with a 2.8 kcal/mol barrier, producing the intermediate **10** (see later discussions for regioselectivity). The coordination of another styrene on **10** gives the intermediate **11**, and **11** undergoes the styrene insertion via **TS12** with the phenyl group of styrene (labeled in red) proximal to the forming C−C bond (see later discussions for regioselectivity). Subsequently, an endergonic styrene coordination on **13** occurs to allow a favorable β-hydride transfer via **TS15**, producing the product-coordinated complex **16**. Complex **16** releases the styrene-dimer product and regenerates the intermediate **10**. The resting state of the whole catalytic cycle is intermediate **13**, and the rate-determining step is the β-hydride transfer via **TS15** with an overall barrier of 15.6 kcal/mol. The initial hydride transfer generates **10** in the first cycle, but thereafter, the β-hydride elimination is coupled to hydride insertion in **TS15**.

In order to address the ligand steric effect on the free-energy profile, we also studied the same reaction pathway with SIPr (1,3-bis(2,6-diisopropylphenyl)-4,5-dihydroimidazol-2-ylidene). The free-energy changes of the desired pathway are very similar to the two ligands (Figure 1 vs Figure 2). With SIPr ligand, the hydride insertion and olefin insertion steps are very facile, leading to the formation of the resting state, **22**. The subsequent β-hydride transfer, via **TS24**, is the rate-limiting step of the catalytic cycle with an overall barrier of 16.1 kcal/mol.

***β*-Hydride Transfer vs *β*-Hydride Elimination.** A previous theoretical study on a similar reaction with a [(R_3P)NiH]$^+$ catalyst found that a β-hydride transfer step,

DOI: 10.1021/acscatal.5b01075
ACS Catal. 2015, 5, 5545−5555

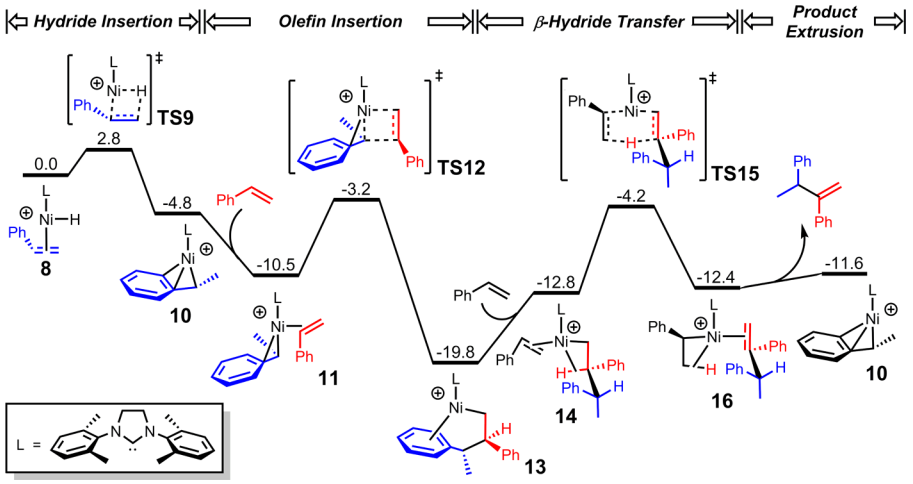

Figure 1. Free-energy changes of the most favorable pathway of [(NHC)NiH]$^+$-catalyzed tail-to-tail dimerization of styrenes (Gibbs free energies in kcal/mol). L = 1,3-bis(2,6-dimethylphenyl)-4,5-dihydroimidazol-2-ylidene.

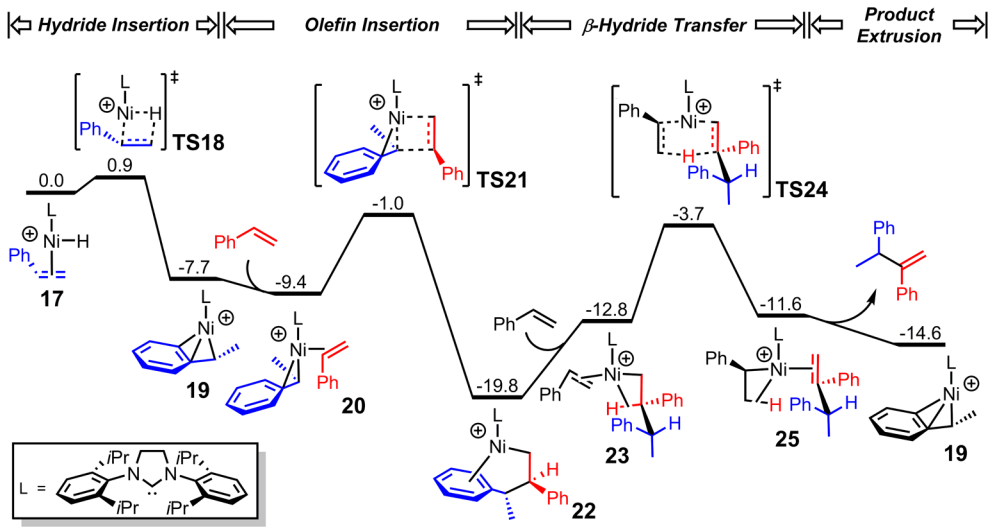

Figure 2. Free-energy changes of the most favorable pathway of [(NHC)NiH]$^+$-catalyzed tail-to-tail dimerization of styrenes (Gibbs free energies in kcal/mol). L = SIPr.

instead of a classic β-hydride elimination step, occurs to generate the hydroalkenylation product.[17c] As found here (Figure 1), these results imply that the hydroalkenylation with [(R_3P)NiH]$^+$ catalysts proceeds without a nickel-hydride species after the catalyst initiation.[23]

With the [(NHC)NiH]$^+$ catalyst, we studied the competition between a β-hydride transfer and a β-hydride elimination. Figure 3 shows that β-hydride transfer step (via **TS15**) is only slightly favored by 0.6 kcal/mol over a β-hydride elimination step (via **TS27**).[24] This is different from the mechanism with phosphorus-based nickel catalyst, in which the β-hydride transfer step is found to be more favorable by about 10 kcal/mol compared with β-hydride elimination step.[17c] The major difference between the NHC and the phosphorus ligand is the barrier of β-hydride elimination. With the phosphorus ligand, the β-hydride elimination generates a very unstable nickel-hydride species, and the step is about 20 kcal/mol endergonic.[17c] This makes the reaction pathway with β-hydride elimination very unfavorable. While with the NHC ligand, the nickel-hydride species, **28**, is significantly stabilized, and the β-hydride elimination from **26** to **28** is only endergonic by 3.1 kcal/mol. The stabilization of nickel-hydride intermediate with NHC ligand makes the β-hydride elimination competitive with the β-hydride transfer. To further confirm the competition between these two steps, we also calculated the competing transition states with SIPr ligand. The β-hydride transfer is also more favorable by only 0.8 kcal/mol than the β-hydride elimination step with SIPr ligand.[25] This suggests that the two steps are competitive with both IMes and IPr ligands.

Regioselectivity. Based on the computed free-energy profile of the proposed mechanism, we studied the competition between the four regioisomeric hydroalkenylation products between styrene and α-olefins, using styrene dimerization as an example (Scheme 4). Because the first hydride insertion step is very facile, the intermediates **10** and **32** are in equilibrium. We found that the olefin insertion step determines the ratio of the four products (**30**, **31**, **36**, and **37**), and only the branched tail-to-tail product **30** is observed experimentally.

The optimized structures and relative Gibbs free energies of the preintermediates and transition states of the regioselectivity-determining step, olefin insertion, are shown in Figure 4. From **8**, the hydride can insert to the terminal carbon of the

DOI: 10.1021/acscatal.5b01075
ACS Catal. 2015, 5, 5545−5555

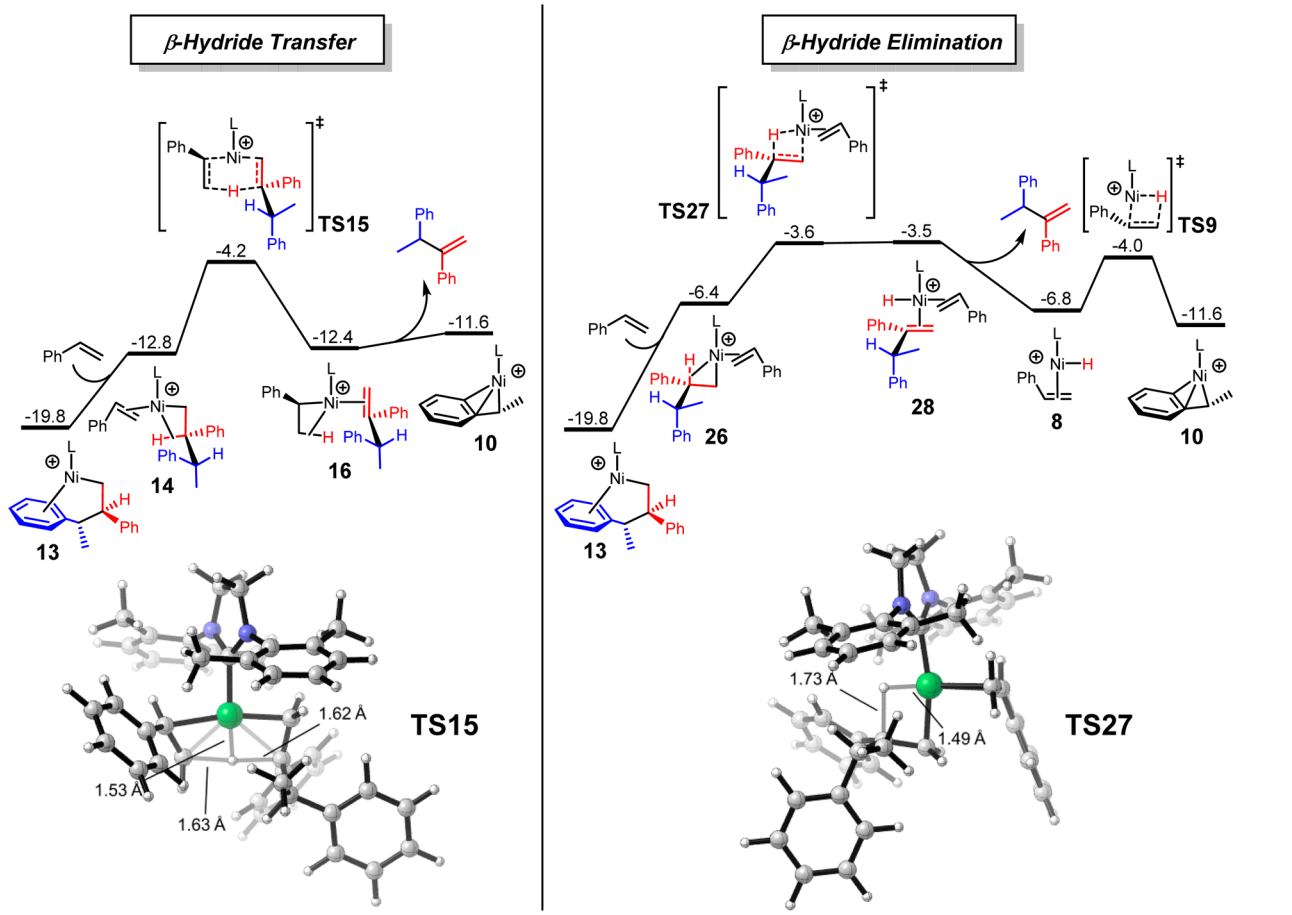

Figure 3. Free-energy changes and transition state structures of β-hydride transfer and β-hydride elimination steps from intermediate **13** (Gibbs free energies in kcal/mol). L = 1,3-bis(2,6-dimethylphenyl)-4,5-dihydroimidazol-2-ylidene.

Scheme 4. Four Possible Regioisomeric Products of [(NHC)NiH]$^+$-Catalyzed Styrene Dimerization

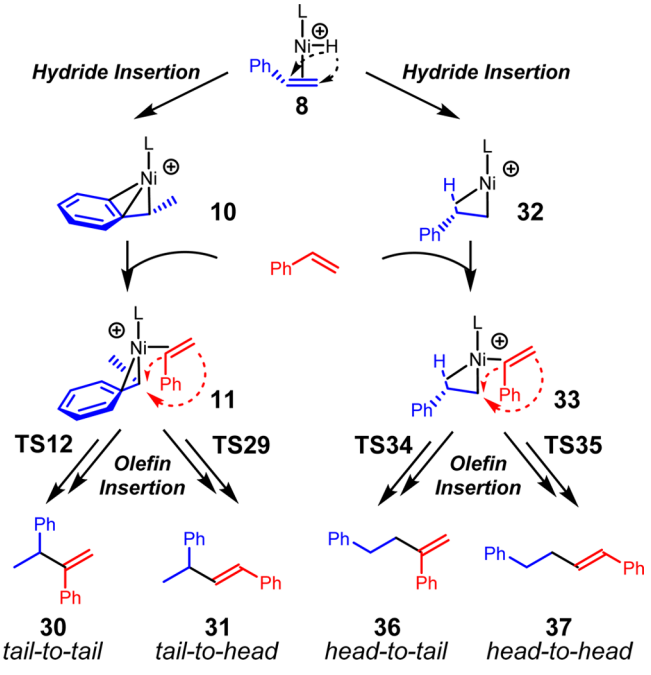

styrene, generating the intermediate **10**, and **10** undergoes a styrene coordination to give the intermediate **11** (Scheme 4). Subsequently, there are two possible styrene insertion transition states, **TS12** and **TS29**, leading to **30** and **31**, respectively. Alternatively, the initial hydride insertion of **8** could occur on the internal carbon of the coordinated styrene to generate intermediate **32**. After the styrene coordination, the intermediate **33** also has two corresponding transition states for styrene insertion, **TS34** or **TS35** to give **36** or **37**. The competition between the four insertion transition states, **TS12**, **TS29**, **TS34**, and **TS35**, determines the regioselectivity.

Comparing the intermediates **11** and **33**, **11** is 7.8 kcal/mol more stable, due to the strong coordination from the phenyl group. Interestingly, similar coordination is impossible in intermediate **33**, because the bulky NHC ligand does not allow the sterically demanding phenyl group to rotate to become proximal to the ligand. Instead, only a weak agostic interaction is found. This difference in coordination still exists when comparing the subsequent insertion transition states (**TS12** and **TS29** vs **TS34** and **TS35**). For the same reason, **TS34** and **TS35** only have a weak agostic interaction and are much less favorable than **TS12** and **TS29**.

Comparing the insertion transition states **TS12** and **TS29**, a 3.4 kcal/mol preference for **TS12** is found, in line with the experimental results that only tail-to-tail products are observed. This selectivity is due to the steric repulsion between the NHC ligand and the phenyl group of the inserting styrene in **TS29**. The NHC ligand has local C2 symmetry, while the phosphine ligand has local C3 symmetry. The anisotropic steric environment of NHC ligands has also been found to play an important

DOI: 10.1021/acscatal.5b01075
ACS Catal. 2015, 5, 5545−5555

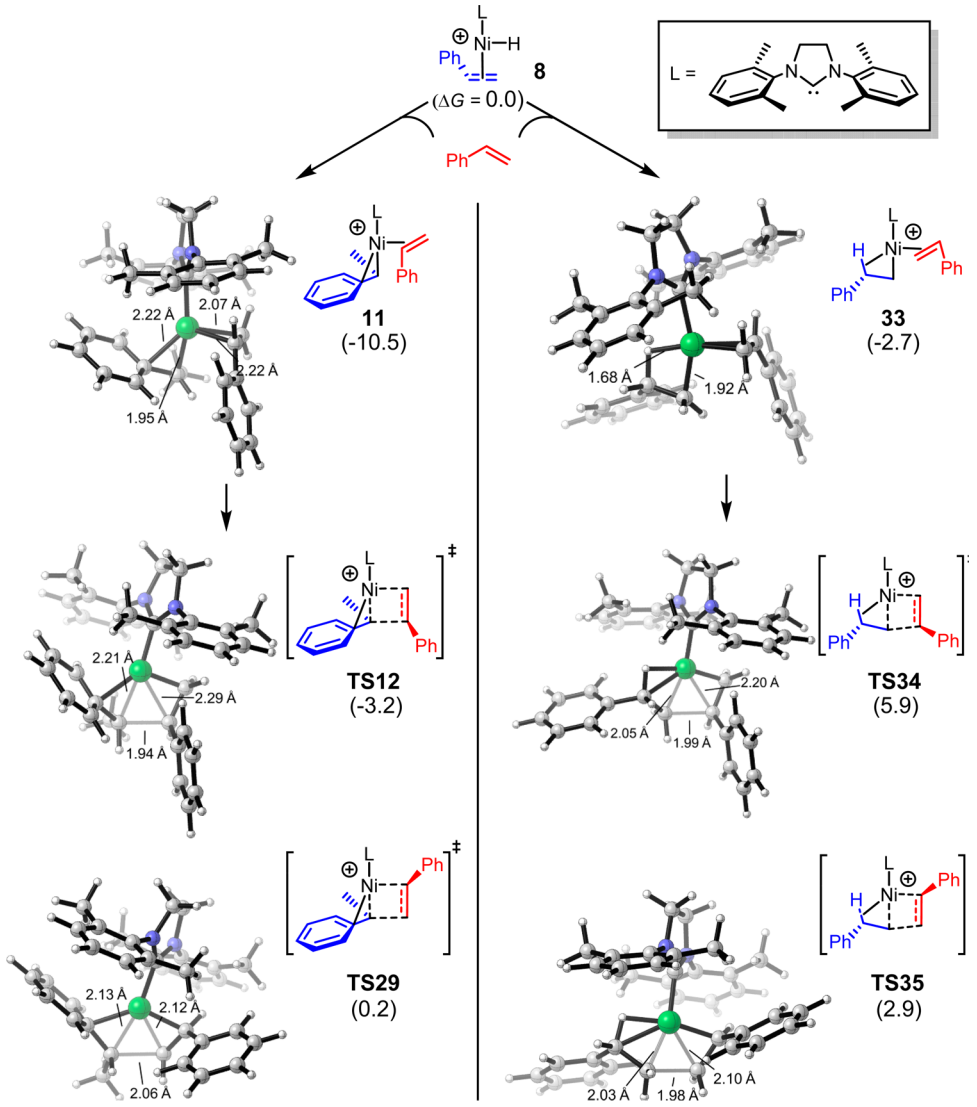

Figure 4. Optimized structures and Gibbs free energies of intermediates and transition states of regioselectivity-determining step, olefin insertion, of [(NHC)NiH]$^+$-catalyzed styrene dimerization (Gibbs free energies in kcal/mol).

role in determining selectivities in other metal-catalyzed reactions with NHC ligands.[26]

To understand the steric effects of ligand on the regioselectivity, we also studied the competition between the four insertion transition states with the SIPr ligand, as shown in Figure 5. The calculated regioselectivities of the SIPr ligand is similar to that of 1,3-bis(2,6-dimethylphenyl)-4,5-dihydroimidazol-2-ylidene. After the initial hydride insertion, the intermediate with phenyl coordination, **20**, is 5.3 kcal/mol more stable than the regioisomeric intermediate **39**. This stabilization of phenyl coordination also differentiates the stabilities of the subsequent olefin insertion transition states, making **TS21** and **TS38** more stable than **TS40** and **TS41**. Comparing **TS21** and **TS38**, we found a 3.4 kcal/mol preference for **TS21**, because of the steric repulsions between the SIPr ligand and the phenyl group of the inserting styrene in **TS38**.

To further understand the regioselectivity, especially the different regioselectivities with NHC and phosphine ligands (Scheme 2), we studied the insertion transition states with various substrates and ligands (results shown in Figure 6). First, the replacement of the inserting styrene by a propene leads to a similar regioselectivity for the tail-to-tail product. **TS42** is 3.5 kcal/mol more stable than **TS43**. This suggests that styrene and other α-olefins have similar tail-to-tail selectivity with bulky NHC ligand, which is consistent with the experimental results.[14a] Changing the *i*Pr groups of the NHC ligand to methyl groups does not affect the regioselectivities significantly, and **TS44** is 3.8 kcal/mol more stable than **TS45**. To understand the intrinsic selectivity and the effects from the steric repulsions of the bulky NHC ligands, we also calculated the selectivity when a small NHC ligand, 1,3-dimethylimidazol-2-ylidene, is used. We found that **TS47**, which gives the tail-to-head product, is now favored by 0.8 kcal/mol compared with **TS46**, indicating a reversed selectivity.[27] Therefore, the tail-to-head product is in fact intrinsically favored, and this intrinsic selectivity is reversed by the bulky NHC ligands. Changing the NHC ligand to triphenylphosphine ligand, the same intrinsic selectivity is found, **TS49** is 1.1 kcal/mol more favorable than **TS48**. The computed selectivity with PPh_3 ligand is also consistent with the previous experiments (Scheme 2).[11,28] This is related to the different steric environments of NHC and phosphine ligands, the cone-shaped phosphorus ligands are not able to alter the intrinsic regioselectivity.

DOI: 10.1021/acscatal.5b01075
ACS Catal. 2015, 5, 5545−5555

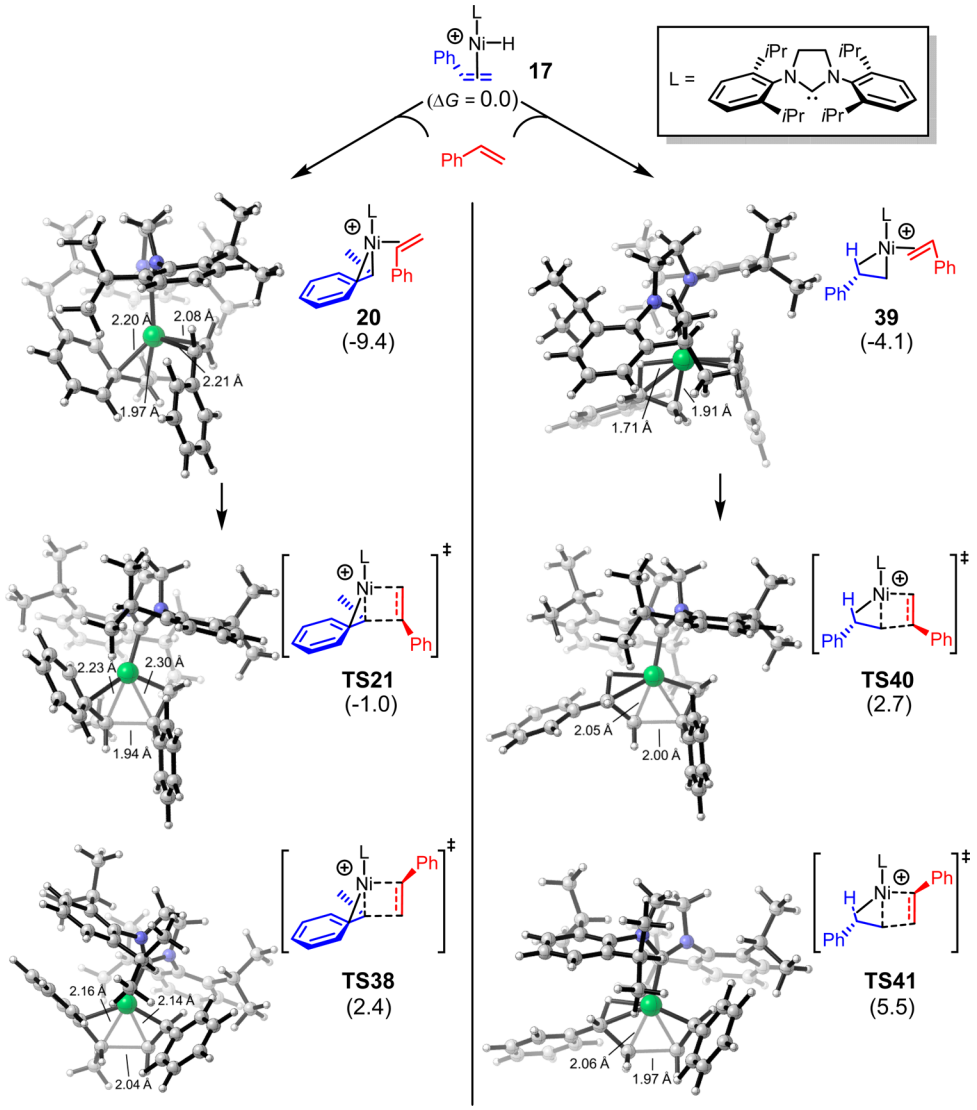

Figure 5. Optimized structures and Gibbs free energies of intermediates and transition states of regioselectivity-determining step, olefin insertion, of [(NHC)NiH]$^+$-catalyzed styrene dimerization (Gibbs free energies in kcal/mol).

Chemoselectivity. We further studied the chemoselectivity of the reaction. In particular, we focused on the following three questions: (1) Why is the heterohydroalkenylation between styrene and α-olefins favored relative to the homodimerization of styrenes? (2) Why is trimerization or further oligomerization of olefins not observed even with excess α-olefins? (3) Why are typical side reactions with α-olefins, such as isomerization and oligomerization, significantly diminished?

Homo- vs Heterohydroalkenylation. The free-energy changes of the pathways that lead to the homo- or the heterohydroalkenylation products are shown in Figure 7. In line with the experimental results that the heterohydroalkenylation is more favorable than the homohydroalkenylation, we found a 2.4 kcal/mol preference to the heterodimerization pathway (**TS44** vs **TS12**). Although the coordination of styrene is stronger than that of propene, and intermediate **11** is 1.6 kcal/mol more stable than **50**. The insertion of styrene breaks the conjugation between the inserting double bond and phenyl group, leading to a higher barrier of insertion, while the insertion of propene or other α-olefins does not need to break such conjugation.[29] To confirm the change of π-conjugation in the insertion, we calculated the distortion of styrene and propene in the competing insertion transition states, **TS12** and **TS44**, as shown in Figure 8. The distortion energies of alkenes are calculated by comparing the gas-phase electronic energies of the distorted alkenes in the transition states (**TS12** and **TS44**) with those of the ground states. As highlighted in Figure 8, styrene and propene are distorted similarly except that the exocyclic double bond of styrene is no longer in the same plane with the phenyl group as in the ground state. This weakens the π-conjugation in styrene and makes the distortion energy of styrene 3.4 kcal/mol larger than that of propene. The change in distortion energy is also comparable to the energy difference in the transition states (**TS12** vs **TS44**), suggesting that the major contribution to the chemoselectivity is the change of π-conjugation in the olefin insertion step.

Dimerization vs Trimerization. The free-energy changes of the dimerization and trimerization pathways were studied by using the styrene only, and the results are shown in Figure 9. From intermediate **14**, the β-hydride transfer via **TS15** gives the styrene-dimer-coordinated complex **16**, and the substrate extrusion and subsequent steps generate the intermediate **13** for the next catalytic cycle. Alternatively, **14** can isomerize to intermediate **26**, which undergoes the styrene insertion via

DOI: 10.1021/acscatal.5b01075
ACS Catal. 2015, 5, 5545−5555

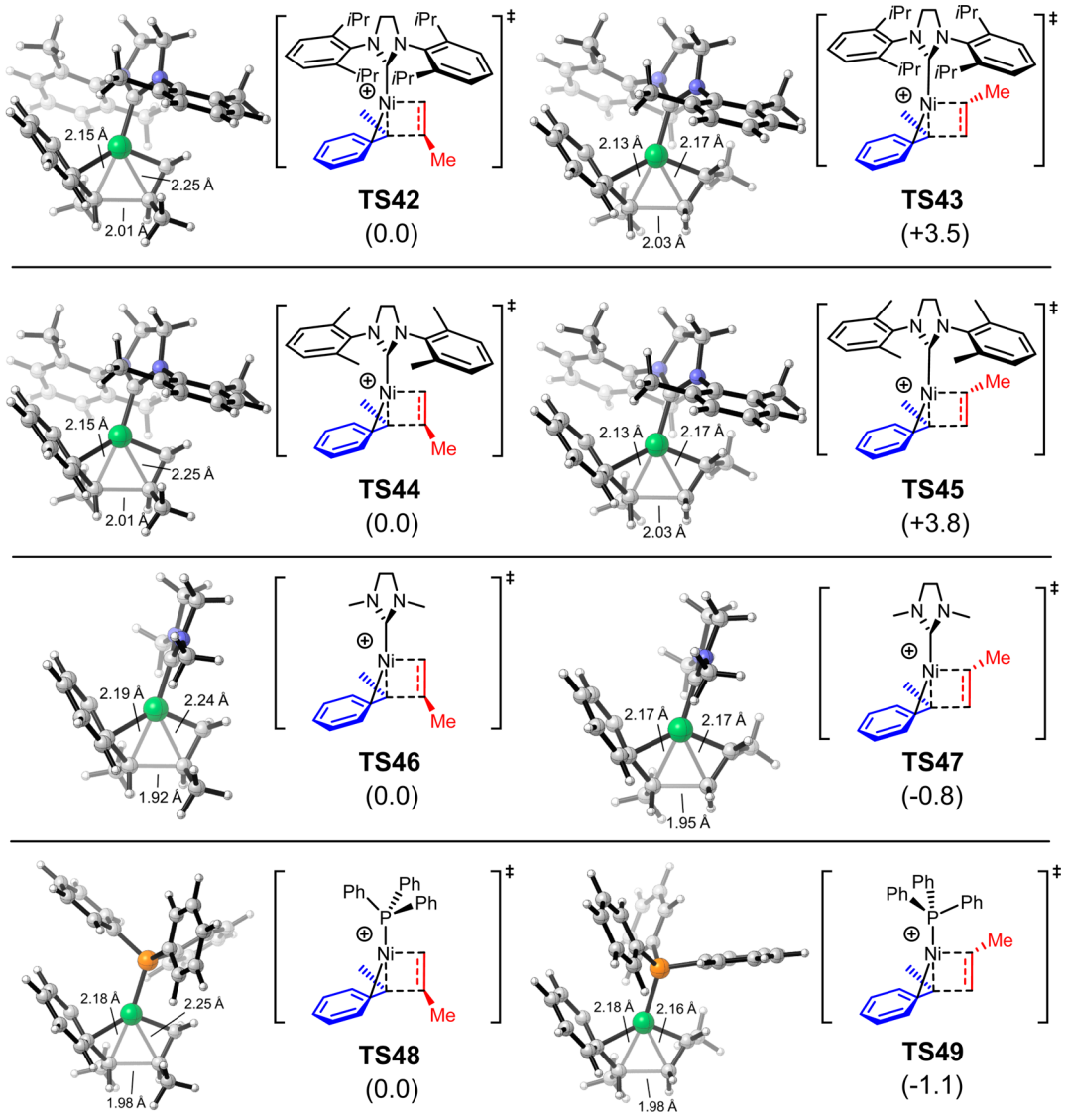

Figure 6. Optimized structures and relative Gibbs free energies of propene insertion transition states with three ligands (Gibbs free energies in kcal/mol).

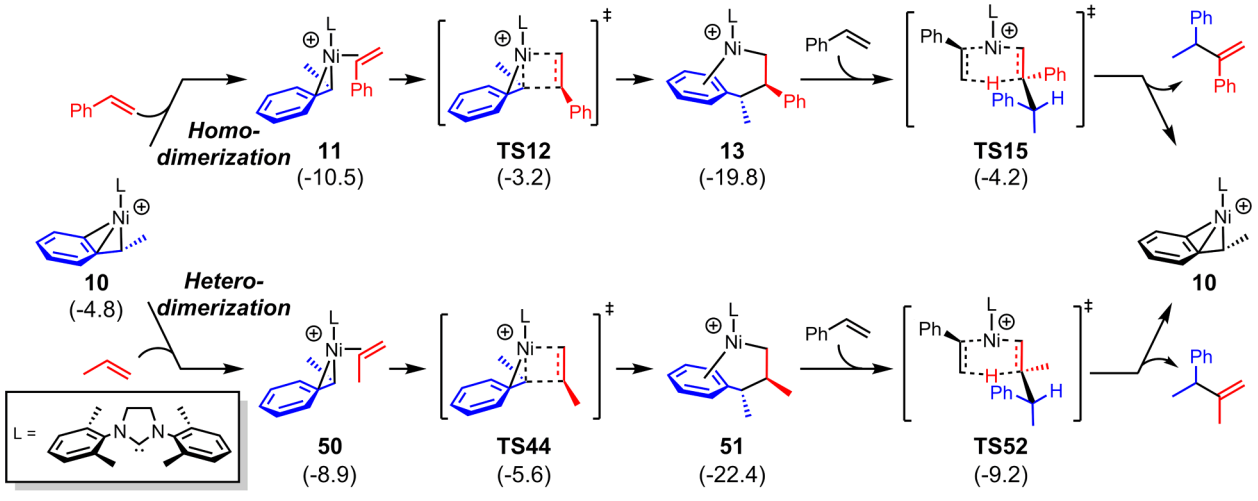

Figure 7. Free-energy profiles of [LNiH]$^+$-catalyzed hydroalkenylation of styrene with styrene or propene (Gibbs free energies with respect to the intermediate **8** are shown in kcal/mol).

DOI: 10.1021/acscatal.5b01075
ACS Catal. 2015, 5, 5545−5555

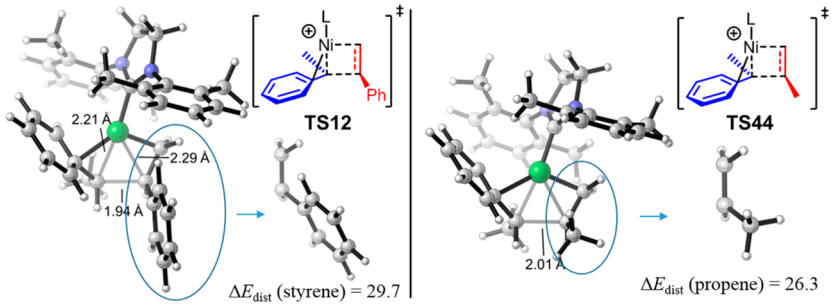

Figure 8. Optimized structures of olefin insertion transition states, **TS12** and **TS44**, and the distortion energies of the inserting alkenes in the transition states. L = 1,3-bis(2,6-dimethylphenyl)-4,5-dihydroimidazol-2-ylidene.

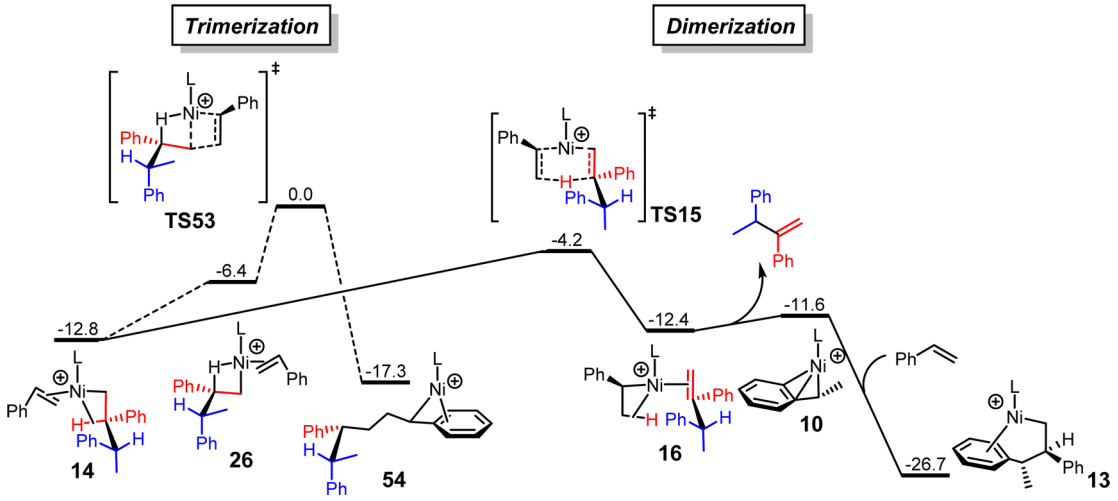

Figure 9. Free-energy changes of the styrene dimerization and trimerization pathways (Gibbs free energies in kcal/mol). L = 1,3-bis(2,6-dimethylphenyl)imidazol-2-ylidene.

TS53 for the trimerization.[30] Because of this endergonic isomerization from **14** to **26**, the styrene trimerization is 4.2 kcal/mol less favorable than the dimerization (**TS53** vs **TS15**). This explains the experimental result that only dimerization occurs with no trimerization or further oligomerization.

Side Reactions with α-Olefins. We also studied the competition between the observed hydroalkenylation with styrene and dimerization of α-olefins. As shown in Figure 10, the propene insertion step via **TS56** requires a 19.2 kcal/mol barrier as compared to the resting state **13**, which is 3.6 kcal/mol higher in free energy than the rate-limiting step of the styrene dimerization via **TS15**. This is mainly because the dimerization of α-olefins, or other side reactions, does not involve any stable transition states or intermediates with a strong Ni-Ph bond like **13**.[31] Therefore, the side reactions with α-olefins are inhibited in the presence of styrene.

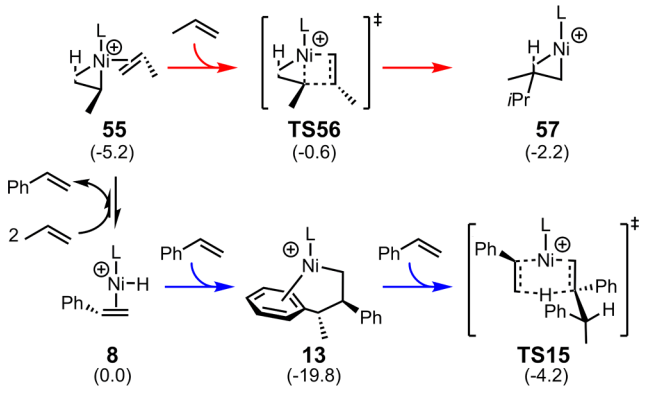

Figure 10. Competition between [(NHC)NiH]$^+$-catalyzed styrene and propene dimerization. L = 1,3-bis(2,6-dimethylphenyl)imidazol-2-ylidene.

Based on the computations, the reactant styrene can also be regarded as an inhibitor of the side reactions with α-olefins. Without styrene, or other vinylarenes that can generate similar stable intermediates like **13**, the side reactions with α-olefins should be favorable.

To test this prediction, we studied 1-octene consumption in the absence of styrene, and we compared the results with the standard reaction in a shorter time (reduced from 24 to 2 h). In the absence of styrene, all of the 1-octene is consumed in undesired nonselective isomerization and homodimerization at a much faster rate (Entry 1, Table 1). In the presence of styrene, only half of the 1-octene was consumed and much fewer undesired processes with 1-octene occurred (Entry 2, Table 1). Thus, nearly half of the 1-octene remained unreacted in the presence of styrene within 2 h. These results clearly showed that the styrene and the products derived were responsible for the suppression of side reactions.

CONCLUSION

The mechanism, chemo- and regioselectivities of [(NHC)-NiH]$^+$-catalyzed hydroalkenylations between styrene and α-olefins have been explored through DFT calculations. From the

DOI: 10.1021/acscatal.5b01075
ACS Catal. 2015, 5, 5545−5555

Table 1. Effect of Styrene and Its Derived Products on the Rate of α-Olefin Consumption in the Reaction with [(NHC)NiH](OTf) Catalyst

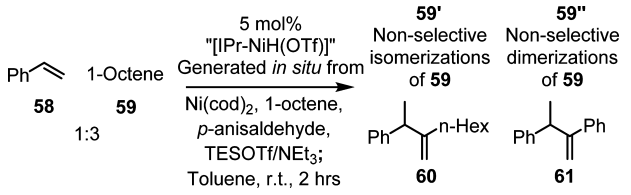

entry[a]	styrene	conversion of 59(%)[b]	yield of 60 + 61 (%) (60:61)[b]	(59′: 59″)[c]
1	no	100	/	73:27
2	yes	50	46 (90:10)	N.D.

[a]The reactions were conducted according to the original paper, except otherwise indicated above. [b]Determined by the NMR ratio. [c]Determined by GC-MS (sum of the area of the nonselective 59′ and 59″), the N.D. was due to overlap of 1-octene and 1-octene isomers.

$[LNiH(styrene)]^+$ intermediate, a facile hydride insertion and subsequent olefin insertion generate the resting state of the catalytic cycle. This intermediate undergoes the rate-limiting β-hydride transfer step to produce the hydroalkenylation product. The olefin insertion step is found to determine the regioselectivity that favors the tail-to-tail product. Only the insertion transition state for the tail-to-tail product is favored both electronically and sterically. This transition state has a strong interaction between nickel and a phenyl group, with the substituent of the inserting asymmetric alkene pointing away from the bulky NHC ligand. The olefin insertion step also determines the chemoselectivity between heterohydroalkenylation and homohydroalkenylation. The insertion of aryl-substituted alkene breaks the conjugation between the inserting double bond and the aryl group, while the insertion of alkyl-substituted alkene does not break such conjugation. This leads to the favorable heterohydroalkenylation with alkyl-substituted alkenes.

The stable resting state of the hydroalkenylation with styrene, which has a strong interaction between nickel and phenyl group, makes the side reactions with α-olefins difficult. This suggests that styrene is not only a substrate but also an inhibitor for the side reactions with other α-olefins. This unique effect of styrene was proved experimentally. When the catalyst was subjected to only 1-octene, nonselective olefin isomerization and dimerization were found, while the heterohydroalkenylation with styrene under the same conditions generates the desired heterodimer as the major product.

■ ASSOCIATED CONTENT

Supporting Information

The Supporting Information is available free of charge on the ACS Publications website at DOI: 10.1021/acscatal.5b01075.

General information on experiments, and experimental procedures. Experimental selectivities with IMes and IPr ligands. Alternative β-hydride elimination and styrene insertion pathway. Competition between β-hydride transfer and β-hydride elimination with SIPr ligand. Coordinates and energies of DFT-computed stationary points (PDF)

■ AUTHOR INFORMATION

Corresponding Authors

*E-mail: jasonhcy@sustc.edu.cn.

*E-mail: houk@chem.ucla.edu.

Author Contributions

All authors have given approval to the final version of the manuscript.

Notes

The authors declare no competing financial interest.

■ ACKNOWLEDGMENTS

K.N.H. thanks the NSF (CHE-1361104) for financial support of this research. Calculations were performed on the Hoffman2 Cluster at UCLA and the Extreme Science and Engineering Discovery Environment (XSEDE), which is supported by the NSF (OCI-1053575). C.Y.H. thanks the Thousand Young Talents Program, SUSTC start up fund, Guangdong Province Matching Fund K12213101, and CUHK for financial support. L.H. acknowledges the HK Ph.D. Fellowship.

■ REFERENCES

(1) For selected reviews on recent developments of C-C bond formations, see: (a) Ritleng, V.; Sirlin, C.; Pfeffer, M. *Chem. Rev.* **2002**, *102*, 1731−1770. (b) Nicolaou, K. C.; Bulger, P. G.; Sarlah, D. *Angew. Chem., Int. Ed.* **2005**, *44*, 4442−4489. (c) Marion, N.; Nolan, S. P. *Acc. Chem. Res.* **2008**, *41*, 1440−1449. (d) Li, C. − J. *Acc. Chem. Res.* **2009**, *42*, 335−344. (e) Colby, D. A.; Bergman, R. G.; Ellman, J. A. *Chem. Rev.* **2010**, *110*, 624−655. (f) Rodriguez, N.; Goossen, L. J. *Chem. Soc. Rev.* **2011**, *40*, 5030−5048. (g) Cho, S. H.; Kim, J. Y.; Kwak, J.; Chang, S. *Chem. Soc. Rev.* **2011**, *40*, 5068−5083. (h) Johansson Seechurn, C. C. C.; Kitching, M. O.; Colacot, T. J.; Snieckus, V. *Angew. Chem., Int. Ed.* **2012**, *51*, 5062−5085. (i) Kumar, R.; Van der Eycken, E. V. *Chem. Soc. Rev.* **2013**, *42*, 1121−1146.

(2) For reviews on hydrovinylation reaction, see: (a) Hilt, G. *Eur. J. Org. Chem.* **2012**, *2012*, 4441−4451. (b) Ceder, R. M.; Grabulosa, A.; Muller, G.; Rocamora, M. *Catal. Sci. Technol.* **2013**, *3*, 1446−1464. (c) Saini, V.; Stokes, B. J.; Sigman, M. S. *Angew. Chem., Int. Ed.* **2013**, *52*, 11206−11220.

(3) Alderson, T.; Jenner, E. L.; Lindsey, R. V., Jr. *J. Am. Chem. Soc.* **1965**, *87*, 5638−5645.

(4) For selected reviews on Ni-catalyzed hydrovinylation, see: (a) Gooβen, L. J. *Angew. Chem., Int. Ed.* **2002**, *41*, 3775−3778. (b) RajanBabu, T. V. *Chem. Rev.* **2003**, *103*, 2845−2860. (c) RajanBabu, T. V. *Synlett* **2009**, *2009*, 853−885. For reviews on related Ni-catalyzed C−H activations, see: (d) Tasker, S. Z.; Standley, E. A.; Jamison, T. F. *Nature* **2014**, *509*, 299−309.

(5) For Ru-catalyzed hydrovinylation, see: (a) Foley, N. A.; Lail, M.; Lee, J. P.; Gunnoe, T. B.; Cundari, T. R.; Petersen, J. L. *J. Am. Chem. Soc.* **2007**, *129*, 6765−6781. (b) Gooßen, L. J.; Rodriguez, N. *Angew. Chem., Int. Ed.* **2007**, *46*, 7544−7546. (c) Kondo, T.; Takagi, D.; Tsujita, H.; Ura, Y.; Wada, K.; Mitsudo, T. *Angew. Chem., Int. Ed.* **2007**, *46*, 5958−5961. (d) Sanchez, R. P., Jr.; Connell, B. T. *Organometallics* **2008**, *27*, 2902−2904. (e) Neisius, N. M.; Plietker, B. *Angew. Chem., Int. Ed.* **2009**, *48*, 5752−5755. (f) Jiang, G.; List, B. *Chem. Commun.* **2011**, *47*, 10022−10024. (g) Saito, N.; Saito, K.; Shiro, M.; Sato, Y. *Org. Lett.* **2011**, *13*, 2718−2721. (h) Wang, Q. − S.; Xie, J. − H.; Li, W.; Zhu, S. − F.; Wang, L. − X.; Zhou, Q. − L. *Org. Lett.* **2011**, *13*, 3388−3391. (i) Yun, S. Y.; Wang, K. − P.; Kim, M.; Lee, D. *J. Am. Chem. Soc.* **2012**, *134*, 10783−10786. (j) Hiroi, Y.; Komine, N.; Komiya, S.; Hirano, M. *Org. Lett.* **2013**, *15*, 2486−2489. (k) Schabel, T.; Plietker, B. *Chem. - Eur. J.* **2013**, *19*, 6938−6941. (l) Simon, M.; Darses, S. *J. Org. Chem.* **2013**, *78*, 9981−9985. (m) Hiroi, Y.; Komine, N.; Komiya, S.; Hirano, M. *Organometallics* **2014**, *33*, 6604−6613.

(6) For Co-catalyzed hydrovinylation, see: (a) Grutters, M. M. P.; Müller, C.; Vogt, D. *J. Am. Chem. Soc.* **2006**, *128*, 7414−7415. (b) Hilt, G.; Treutwein, J. *Chem. Commun.* **2009**, 1395−1397. (c) Grutters, M.

DOI: 10.1021/acscatal.5b01075
ACS Catal. 2015, 5, 5545−5555

M. P.; van der Vlugt, J. I.; Pei, Y.; Mills, A. M.; Lutz, M.; Spek, A. L.; Müller, C.; Moberg, C.; Vogt, D. *Adv. Synth. Catal.* **2009**, *351*, 2199−2208. (d) Vogt, D. *Angew. Chem., Int. Ed.* **2010**, *49*, 7166−7168. (e) Arndt, M.; Reinhold, A.; Hilt, G. *J. Org. Chem.* **2010**, *75*, 5203−5210. (f) Arndt, M.; Dindaroglu, M.; Schmalz, H.; Hilt, G. *Org. Lett.* **2011**, *13*, 6236−6239. (g) Kersten, L.; Hilt, G. *Adv. Synth. Catal.* **2012**, *354*, 863−869. (h) Timsina, Y. N.; Biswas, S.; RajanBabu, T. V. *J. Am. Chem. Soc.* **2014**, *136*, 6215−6218.

(7) For Pd-catalyzed hydrovinylation, see: (a) Shi, W. − J.; Xie, J. − H.; Zhou, Q. − L. *Tetrahedron: Asymmetry* **2005**, *16*, 705−710. (b) Ayora, I.; Ceder, R. M.; Espinel, M.; Muller, G.; Rocamora, M.; Serrano, M. *Organometallics* **2011**, *30*, 115−128. (c) Choi, J. H.; Kwon, J. K.; RajanBabu, T. V.; Lim, H. J. *Adv. Synth. Catal.* **2013**, *355*, 3633−3638. (d) Carrilho, R. M. B.; Costa, G. N.; Neves, Â. C. B.; Pereira, M. M.; Grabulosa, A.; Bayón, J. C.; Rocamora, M.; Muller, G. *Eur. J. Inorg. Chem.* **2014**, *2014*, 1034−1041.

(8) For Rh-catalyzed hydrovinylation, see: (a) Hölscher, M.; Uhe, A.; Leitner, W. *J. Organomet. Chem.* **2013**, *748*, 13−20. (b) Azpíroz, R.; Rubio-Pérez, L.; Di Giuseppe, A.; Passarelli, V.; Lahoz, F. J.; Castarlenas, R.; Pérez-Torrente, J. J.; Oro, L. A. *ACS Catal.* **2014**, *4*, 4244−4253.

(9) For Pt-catalyzed hydrovinylation, see: (a) Serra, D.; Cao, P.; Cabrera, J.; Padilla, R.; Rominger, F.; Limbach, M. *Organometallics* **2011**, *30*, 1885−1895.

(10) (a) Bogdanović, B.; Henc, B.; Meister, B.; Pauling, H.; Wilke, G. *Angew. Chem., Int. Ed. Engl.* **1972**, *11*, 1023−1024. (b) Bogdanović, B.; Henc, B.; Meister, B.; Pauling, H.; Wilke, G. *Angew. Chem., Int. Ed. Engl.* **1973**, *12*, 954−964. (c) Wilke, G. *Angew. Chem., Int. Ed. Engl.* **1988**, *27*, 185−206.

(11) (a) RajanBabu, T. V.; Ayers, T. A.; Halliday, G. A.; You, K. K.; Calabrese, J. C. *J. Org. Chem.* **1997**, *62*, 6012−6028. (b) Park, H.; RajanBabu, T. V. *J. Am. Chem. Soc.* **2002**, *124*, 734−735. (c) Kumareswaran, R.; Nandi, N.; RajanBabu, T. V. *Org. Lett.* **2003**, *5*, 4345−4348. (d) RajanBabu, T. V.; Nomura, N.; Jin, J.; Nandi, M.; Park, H.; Sun, X. *J. Org. Chem.* **2003**, *68*, 8431−8446. (e) Zhang, A.; RajanBabu, T. V. *J. Am. Chem. Soc.* **2006**, *128*, 54−55. (f) Zhang, A.; RajanBabu, T. V. *J. Am. Chem. Soc.* **2006**, *128*, 5620−5621. (g) Saha, B.; RajanBabu, T. V. *Org. Lett.* **2006**, *8*, 4657−4659. (h) Saha, B.; RajanBabu, T. V. *J. Org. Chem.* **2007**, *72*, 2357−2363. (i) Smith, C. R.; Mans, D.; RajanBabu, T. V. *Org. Synth.* **2008**, *85*, 238−247. (j) Saha, B.; Smith, C. R.; RajanBabu, T. V. *J. Am. Chem. Soc.* **2008**, *130*, 9000−9005. (k) Smith, C. R.; RajanBabu, T. V. *Org. Lett.* **2008**, *10*, 1657−1659. (l) Smith, C. R.; RajanBabu, T. V. *J. Org. Chem.* **2009**, *74*, 3066−3072. (m) Smith, C. R.; Lim, H. J.; Zhang, A.; RajanBabu, T. V. *Synthesis* **2009**, *12*, 2089−2100. (n) Liu, W.; RajanBabu, T. V. *J. Org. Chem.* **2010**, *75*, 7636−7643. (o) Sharma, R. S.; RajanBabu, T. V. *J. Am. Chem. Soc.* **2010**, *132*, 3295−3297. (p) Mans, D. J.; Cox, G. A.; RajanBabu, T. V. *J. Am. Chem. Soc.* **2011**, *133*, 5776−5779. (q) Liu, W.; Lim, H. J.; RajanBabu, T. V. *J. Am. Chem. Soc.* **2012**, *134*, 5496−5499. (r) Page, J. P.; RajanBabu, T. V. *J. Am. Chem. Soc.* **2012**, *134*, 6556−6559. (s) Biswas, S.; Zhang, A.; Raya, B.; RajanBabu, T. V. *Adv. Synth. Catal.* **2014**, *356*, 2281−2292.

(12) (a) Wegner, A.; Leitner, W. *Chem. Commun.* **1999**, 1583−1584. (b) Franciò, G.; Faraone, F.; Leitner, W. *J. Am. Chem. Soc.* **2002**, *124*, 736−737. (c) Böing, C.; Franciò, G.; Leitner, W. *Chem. Commun.* **2005**, 1456−1458. (d) Böing, C.; Franciò, G.; Leitner, W. *Adv. Synth. Catal.* **2005**, *347*, 1537−1541. (e) Diez-Holz, C. J.; Böing, C.; Franciò, G.; Hölscher, M.; Leitner, W. *Eur. J. Org. Chem.* **2007**, *2007*, 2995−3002. (f) Böing, C.; Hahne, J.; Franciò, G.; Leitner, W. *Adv. Synth. Catal.* **2008**, *350*, 1073−1080. (g) Lassauque, N.; Franciò, G.; Leitner, W. *Eur. J. Org. Chem.* **2009**, *2009*, 3199−3202. (h) Lassauque, N.; Franciò, G.; Leitner, W. *Adv. Synth. Catal.* **2009**, *351*, 3133−3138. (i) Schmitkamp, M.; Leitner, W.; Franciò, G. *Catal. Sci. Technol.* **2013**, *3*, 589−594.

(13) (a) Shi, W. − J.; Zhang, Q.; Xie, J. − H.; Zhu, S. − F.; Hou, G. − H.; Zhou, Q. − L. *J. Am. Chem. Soc.* **2006**, *128*, 2780−2781. (b) Zhang, Q.; Zhu, S. F.; Qiao, X. C.; Wang, L. X.; Zhou, Q. L. *Adv. Synth. Catal.* **2008**, *350*, 1507−1510.

(14) For Ho's work, see: (a) Ho, C. − Y.; He, L. *Angew. Chem., Int. Ed.* **2010**, *49*, 9182−9186. (b) Ho, C. − Y.; He, L.; Chan, C. − W. *Synlett* **2011**, *2011*, 1649−1653. (c) Ho, C. − Y.; He, L. *Chem. Commun.* **2012**, *48*, 1481−1483. (d) He, L.; Ho, C. − Y. *Synlett* **2014**, *25*, 2738−2742. (e) Ho, C. − Y.; He, L. *J. Org. Chem.* **2014**, *79*, 11873−11884. For related transformations with nickel catalysts, see: (f) Ho, C.-Y.; Jamison, T. F. *Angew. Chem., Int. Ed.* **2007**, *46*, 782−785. (g) Ho, C.-Y.; Ohmiya, H.; Jamison, T. F. *Angew. Chem., Int. Ed.* **2008**, *47*, 1893−1895. (h) Matsubara, R.; Jamison, T. F. *J. Am. Chem. Soc.* **2010**, *132*, 6880−6881. (i) Matsubara, R.; Gutierrez, A. C.; Jamison, T. F. *J. Am. Chem. Soc.* **2011**, *133*, 19020−19023. (j) Sergeev, A. G.; Hartwig, J. F. *Science* **2011**, *332*, 439−443. (k) Standley, E. A.; Jamison, T. F. *J. Am. Chem. Soc.* **2013**, *135*, 1585−1592. (l) Tasker, S. Z.; Gutierrez, A. C.; Jamison, T. F. *Angew. Chem., Int. Ed.* **2014**, *53*, 1858−1861. (m) Bair, J. S.; Schramm, Y.; Sergeev, A. G.; Clot, E.; Eisenstein, O.; Hartwig, J. F. *J. Am. Chem. Soc.* **2014**, *136*, 13098−13101.

(15) The detailed chemo- and regioselectivities with IMes and IPr ligands are included in the Supporting Information. These results are previously reported in ref 14a.

(16) Jin, J.; RajanBabu, T. V. *Tetrahedron* **2000**, *56*, 2145−2151.

(17) (a) Bhalla, G.; Oxgaard, J.; Goddard, W. A.; Periana, R. A. *Organometallics* **2005**, *24*, 5499−5502. (b) Oxgaard, J.; Bhalla, G.; Periana, R. A.; Goddard, W. A. *Organometallics* **2006**, *25*, 1618−1625. (c) Joseph, J.; RajanBabu, T. V.; Jemmis, E. D. *Organometallics* **2009**, *28*, 3552−3566.

(18) Frisch, M. J.; Trucks, G. W.; Schlegel, H. B.; Scuseria, G. E.; Robb, M. A.; Cheeseman, J. R.; Scalmani, G.; Barone, V.; Mennucci, B.; Petersson, G. A.; Nakatsuji, H.; Caricato, M.; Li, X.; Hratchian, H. P.; Izmaylov, A. F.; Bloino, J.; Zheng, G.; Sonnenberg, J. L.; Hada, M.; Ehara, M.; Toyota, K.; Fukuda, R.; Hasegawa, J.; Ishida, M.; Nakajima, T.; Honda, Y.; Kitao, O.; Nakai, H.; Vreven, T.; Mont-gomery, J. A., Jr.; Peralta, J. E.; Ogliaro, F.; Bearpark, M.; Heyd, J. J.; Brothers, E.; Kudin, K. N.; Staroverov, V. N.; Keith, T.; Kobayashi, R.; Normand, J.; Raghavachari, K.; Rendell, A.; Burant, J. C.; Iyengar, S. S.; Tomasi, J.; Cossi, M.; Rega, N.; Millam, J. M.; Klene, M.; Knox, J. E.; Cross, J. B.; Bakken, V.; Adamo, C.; Jaramillo, J.; Gomperts, R.; Stratmann, R. E.; Yazyev, O.; Austin, A. J.; Cammi, R.; Pomelli, C.; Ochterski, J. W.; Martin, R. L.; Morokuma, K.; Zakrzewski, V. G.; Voth, G. A.; Salvador, P.; Dannenberg, J. J.; Dap-prich, S.; Daniels, A. D.; Farkas, O.; Foresman, J. B.; Ortiz, J. V.; Cioslowski, J.; Fox, D. J.; *Gaussian 09*, revision D.01; Gaussian, Inc.: Wallingford, CT, 2013.

(19) (a) Zhao, Y.; Truhlar, D. G. *Theor. Chem. Acc.* **2008**, *120*, 215. (b) Zhao, Y.; Truhlar, D. G. *Acc. Chem. Res.* **2008**, *41*, 157−167.

(20) Marenich, A. V.; Cramer, C. J.; Truhlar, D. G. *J. Phys. Chem. B* **2009**, *113*, 6378−6396.

(21) For mechanistic studies on $[LNiH]^+$-catalyzed hydroalkenylation, see: (a) Hölscher, M.; Franciò, G.; Leitner, W. *Organometallics* **2004**, *23*, 5606−5617. (b) Ahlquist, M.; Fabrizi, G.; Cacchi, S.; Norrby, P. *J. Am. Chem. Soc.* **2006**, *128*, 12785−12793. (c) Roy, D.; Sunoj, R. B. *Org. Biomol. Chem.* **2010**, *8*, 1040−1051. (d) Rajeev, R.; Sunoj, R. B. *Dalton Trans.* **2012**, *41*, 8430−8440. For other related computational studies on Ni-catalyzed reactions, see: (e) Musaev, D. G.; Froese, R. D. J.; Svensson, M.; Morokuma, K. *J. Am. Chem. Soc.* **1997**, *119*, 367−374. (f) Deng, L.; Margl, P.; Ziegler, T. *J. Am. Chem. Soc.* **1997**, *119*, 1094−1100. (g) Deng, L.; Woo, T. K.; Cavallo, L.; Margl, P. M.; Ziegler, T. *J. Am. Chem. Soc.* **1997**, *119*, 6177−6186. (h) Normand, A. T.; Hawkes, K. J.; Clement, N. D.; Cavell, K. J.; Yates, B. F. *Organometallics* **2007**, *26*, 5352−5363. (i) Nikiforidis, I.; Görling, A.; Hieringer, W. *J. Mol. Catal. A: Chem.* **2011**, *341*, 63−70.

(22) The IMes and IPr ligands both work in $[(NHC)NiH]^+$-catalyzed hydroalkenylation between styrene and *n*-octene with similar chemo- and regioselectivities.[14a,15] Detailed experimental results with these two ligands are included in the Supporting Information.

(23) For related Ni-catalyzed C−H activation involving nickel-hydride species, see: (a) Shiota, H.; Ano, Y.; Aihara, Y.; Fukumoto, Y.; Chatani, N. *J. Am. Chem. Soc.* **2011**, *133*, 14952−14955. (b) Cornella, J.; Gomez-Bengoá, E.; Martin, R. *J. Am. Chem. Soc.* **2013**, *135*, 1997−2009. (c) Aihara, Y.; Chatani, N. *J. Am. Chem. Soc.* **2013**, *135*, 5308−

DOI: 10.1021/acscatal.5b01075
ACS Catal. 2015, 5, 5545−5555

5311. (d) Song, W.; Ackermann, L. *Chem. Commun.* **2013**, *49*, 6638−6640. (e) Li, M.; Dong, J.; Huang, X.; Li, K.; Wu, Q.; Song, F.; You, J. *Chem. Commun.* **2014**, *50*, 3944−3946. (f) Aihara, Y.; Chatani, N. *J. Am. Chem. Soc.* **2014**, *136*, 898−901. (g) Wu, X.; Zhao, Y.; Ge, H. *J. Am. Chem. Soc.* **2014**, *136*, 1789−1792. (h) Song, W.; Lackner, S.; Ackermann, L. *Angew. Chem., Int. Ed.* **2014**, *53*, 2477−2480.

(24) The barrier of β-hydride elimination has no significant change if nickel is coordinated with other α-olefins. Detailed results are included in the Supporting Information.

(25) The optimized structures of the competing transition states with SIPr ligand are included in the Supporting Information. For a related hydride transfer step in nickel catalysis, see: Guihaumé, J.; Halbert, S.; Eisenstein, O.; Perutz, R. N. *Organometallics* **2012**, *31*, 1300−1314.

(26) (a) Díez-González, S.; Marion, N.; Nolan, S. P. *Chem. Rev.* **2009**, *109*, 3612−3676. (b) Hong, X.; Liu, P.; Houk, K. N. *J. Am. Chem. Soc.* **2013**, *135*, 1456−1462.

(27) In experiment, this small NHC ligand gives the C−C reductive elimination product between the NHC ligand and styrene at elevated temperature, see: Cavell, K. J.; McGuinness, D. S. *Coord. Chem. Rev.* **2004**, *248*, 671−681.

(28) Faissner, R.; Huttner, G. *Eur. J. Inorg. Chem.* **2003**, *2003*, 2239−2244.

(29) For a related phenomenon in rhodium-mediated allene insertion, see: Hong, X.; Stevens, M. C.; Liu, P.; Wender, P. A.; Houk, K. N. *J. Am. Chem. Soc.* **2014**, *136*, 17273−17283.

(30) The regioisomeric insertion of styrene is less favorable, and detailed results are included in the Supporting Information.

(31) Attempts to isolate or observe the resting state (**13** or **51**) by NMR were not successful.

DOI: 10.1021/acscatal.5b01075
ACS Catal. 2015, 5, 5545−5555